

B.I. Kuznetsov, T.B. Nikitina, I.V. Bovdui, K.V. Chunikhin, V.V. Kolomiets, B.B. Kobylanskyi

Method for prediction and control by uncertain microsatellite magnetic cleanliness based on calculation and compensation magnetic field spatial harmonics

Aim. Development of method for prediction and control the microsatellite magnetic cleanliness taking into account the uncertainties of the magnetic characteristics of the microsatellite, based on calculation the magnetic field spatial spherical harmonics in the area of the onboard magnetometer installation and using compensating multipoles. **Methodology.** Spatial spherical harmonics of microsatellite magnetic field in the area of the onboard magnetometer installation calculated as solution of nonlinear minimax optimization problem based on near field measurements for prediction far spacecraft magnetic field magnitude. Nonlinear objective function calculated as the weighted sum of squared residuals between the measured and predicted magnetic field. Values of the compensating dipoles, quadrupoles and octupoles and coordinates of them placement inside the spaceship for compensation of the dipoles, quadrupoles and octupoles components of the microsatellite initial magnetic field also calculated as solution of nonlinear minimax optimization problem. Both solutions of this nonlinear minimax optimization problems calculated based on particle swarm nonlinear optimization algorithms. **Results.** Results of prediction spacecraft far magnetic field magnitude based on spacecraft spatial spherical harmonics of the magnetic field using near field measurements and compensation of the dipoles, quadrupoles and octupoles components of the initial magnetic field with consideration of spacecraft magnetic characteristics uncertainty for ensuring the microsatellite magnetic cleanliness. **Originality.** The method for prediction and control by spacecraft magnetic cleanliness based on calculation spatial spherical harmonics of the magnetic field in the area of the onboard magnetometer installation using compensation of the dipoles, quadrupoles and octupoles components of the initial magnetic field with consideration of magnetic characteristics uncertainty is developed. **Practical value.** The important practical problem of ensuring the magnetic cleanliness of the «Sich-2» microsatellite family based on the spatial spherical harmonics of the magnetic field model using the compensation of the dipole, quadrupole and octupole components of the output magnetic field of the sensor for the kinetic parameters of the neutral component of the space plasma at the point of installation of the on-board magnetometer LEMI-016 by setting the compensating dipole, quadrupole and octupole with consideration of spacecraft magnetic characteristics uncertainty solved. References 59, figures 2.

Key words: microsatellite, magnetic cleanliness, magnetic field spatial spherical harmonics, prediction, control, measurements, uncertainty.

Мета. Розробка методу прогнозування та управління магнітною чистотою мікросупутника на основі обчислення просторових сферичних гармонік магнітного поля в зоні встановлення бортового магнітометру з використанням компенсації сферичних гармонік вихідного магнітного поля та з урахуванням невизначеності магнітних характеристик. **Методологія.** Просторові сферичні гармоніки магнітного поля мікросупутника розраховані як рішення задачі нелінійної мінімаксної оптимізації на основі вимірювань ближнього магнітного поля для прогнозування величини дальнього магнітного поля. Нелінійна цільова функція обчислена в вигляді зваженої суми квадратів залишків між вимірним і прогнозованим магнітним полем. Величини компенсуючих диполів, квадруполів та октуполів та координати їх розташування в просторі мікросупутника для компенсації вихідного магнітного поля космічного апарату розраховані як рішення нелінійної задачі мінімаксної оптимізації. Рішення обох задач нелінійної мінімаксної оптимізації розраховані на основі алгоритмів нелінійної оптимізації роєм частинок. **Результати.** Результати прогнозування величини дальнього магнітного поля мікросупутника на основі обчислення просторових сферичних гармонік моделі магнітного поля в зоні встановлення бортового магнітометру з використанням вимірювань ближнього поля та компенсації дипольних, квадрупольних та октупольних компонент вихідного магнітного поля з урахуванням невизначеності магнітних характеристик для забезпечення магнітної чистоти мікросупутника. **Оригінальність.** Розроблено метод прогнозування та управління магнітною чистотою мікросупутника на основі обчислення просторових сферичних гармонік магнітного поля з використанням компенсації дипольних, квадрупольних та октупольних компонент вихідного магнітного поля та з урахуванням невизначеності магнітних характеристик. **Практична цінність.** Вирішено важливу практичну задачу забезпечення магнітної чистоти орбітального космічного апарату сімейства «Січ-2» на основі обчислення просторових сферичних гармонік моделі магнітного поля з використанням компенсації дипольних, квадрупольних та октупольних компонент вихідного магнітного поля датчика кінетичних параметрів нейтрального компонента космічної плазми в точці розташування бортового магнітометру LEMI-016 шляхом установки компенсуючих диполів, квадруполів та октуполів та з урахуванням невизначеності магнітних характеристик. Бібл. 59, рис. 2.

Ключові слова: космічний апарат, магнітна чистота, просторові сферичні гармоніки магнітного поля, прогнозування, керування, вимірювання, невизначеність.

Introduction. To model the satellites magnetic field the multi-dipole model is currently the most widely used [1 – 14]. On the basis of such a model, the magnetic moment satellite calculated and the magnetic field satellite calculated with sufficient accuracy for practice at a distance greater than three satellites dimensions. Such a model is quite adequate for satellites in which the onboard magnetometer is mounted on a sufficiently long rod. In particular, the length of the rod of the onboard magnetometer of the Danish «Oersted» satellite is 8 m [15]. On «MicroSAT» spacecraft with the «IonoSAT-Micro» instrumentation on-board magnetometer and three wave probes are fixed on the rods lengths are 2 m [16]. However, spacecraft designers are constantly striving to reduce the length of this rod. In particular, on the «Sich-2» family, «CubeSAT» spacecraft onboard magnetometer located inside the spacecraft [17, 18].

Figure 1 shows the location of the sensor of the kinetic parameters of the neutral component of the space plasma (KPNCS) of the «Potential» scientific equipment complex and onboard magnetometer LEMI-016 on the «Sich-2» spacecraft [18].

In particular, on the «Sich-2» spacecraft family onboard magnetometer LEMI-016 is located at a distance of 0.35 m from the sensor KPNCS [18]. The principle of operation of this sensor is based on the use of the force effect of a magnetic field on an electrically neutral component of space plasma. In this case, permanent magnets are used to create an internal magnetic field in the sensor.

Therefore, the standard of the European Space Agency ECSS-E-20A limits the value of the magnetic field spacecraft units at a distance of 0.1 m from their surface [19]. Therefore, to model the magnetic field of

such satellites, it is necessary to use a multipole model based on spatial harmonics [20–26].

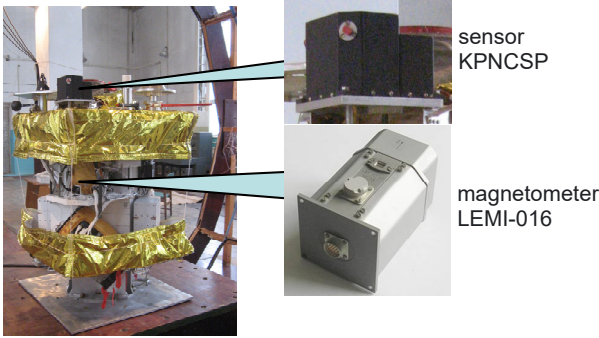


Fig. 1. Location of the sensor of the KPNCSP and onboard magnetometer LEMI-016 on the «Sich-2» spacecraft

In addition, in the course of spacecraft assembly, to compensate for the satellite units magnetic moments, such a spatial arrangement of these units is often used so that the total magnetic moment would be equal to zero. To compensate for the spacecraft units magnetic moments, as well as to compensate for the residual magnetic moments of the entire spacecraft, compensating magnetic units are used. As a result of such measures, it is possible to reduce the magnitudes of the units magnetic moments and the entire spacecraft to sufficiently small values. However, as a result of these measures, quadrupole, octupole and harmonics of a higher order appear, so that the level of the magnetic field near the satellite surface determined mainly by quadrupole, octupole, etc. harmonics.

In particular, in the practice of spacecraft designing to compensate for the dipole magnetic moments of electromagnetic relays, they are often installed in pairs next to each other, so that such a design becomes a quadrupole magnetic field source. To compensate for the dipole magnetic moments of high-frequency gate switch, they are often installed side by side in fours, six or even eight elements. This design becomes a quadrupole, octupole, and even higher order magnetic field source.

To reduce the magnetic moment of the sensor of the neutral component of the plasma, which is part of the scientific equipment of the «Sich-2» spacecraft, an antisymmetric orientation of permanent magnets and a ferromagnetic screen are used. In this case [18], the magnetic moment of the sensor of the neutral component of the plasma generates only 20 % of the induction at the installation point of the onboard magnetometer LEMI-016, and the remaining 80 % of the induction generates by the a quadrupole and octupole – second and third spatial harmonics of the magnetic field of the sensor of the neutral component of the plasma.

Therefore, for an adequate description of the magnetic field in the satellite near zone it is necessary to use a multipole model, including a quadrupole, octupole, and, possibly, a higher order model of the satellite's magnetic field. The European Space Agency ECSS-E-HB-20-07A also recommends using spherical harmonics as integral characteristics of the magnetic field to improve the satellites magnetic cleanliness [19].

In addition, the characteristics of the magnetic cleanliness of the spacecraft units change when their operating modes change and during the flight. Therefore, the European Space Agency recommends testing the units and the entire spacecraft in various modes of operation [19].

The aim of the work is to develop a method for prediction and control the microsatellite magnetic cleanliness taking into account the uncertainties of the magnetic characteristics of the microsatellite, based on calculation the magnetic field spatial harmonics in the area of the onboard magnetometer installation and using compensating multipole.

Model of spatial spherical harmonics microsatellite magnetic field. When design a mathematical model of the microsatellite magnetic field the Gauss equation for the scalar magnetic potential of the source in the surrounding space written in spherical coordinates r , φ and θ in the following form [2]:

$$U = \frac{1}{4\pi} \cdot \sum_{n=1}^{\infty} \left(\frac{1}{r}\right)^{n+1} \cdot \sum_{m=0}^n (g_n^m \cdot \cos m\varphi + \dots) \quad (1)$$

$$\dots + h_n^m \cdot \sin m\varphi) \cdot P_n^m(\cos \theta),$$

where r is the radius of the sphere on which the potential is determined; g_n^m , h_n^m – constant coefficients.

Then from (1) the components B_r , B_φ , B_θ of the magnetic field in the spherical coordinate system r , φ and θ associated with the geometric center of the microsatellite calculated (2).

To ensure the microsatellite magnetic field cleanliness the European Space Agency ECSS-E-HB-20-07A recommends [19] used spatial harmonics up to octupole harmonics as characteristics of the microsatellite magnetic field cleanliness. In addition to the microsatellite magnetic moment, which is characterized by three components g_1^0 , g_1^1 , h_1^1 in (1), it is necessary to determine five more coefficients g_2^0 , g_2^1 , g_2^2 , h_2^1 , h_2^2 for the quadrupole component and seven coefficients g_3^0 , g_3^1 , g_3^2 , g_3^3 , h_3^1 , h_3^2 , h_3^3 octupole component of the magnetic field spherical harmonics:

$$B_r = \frac{\mu_0}{4\pi} \cdot \sum_{n=1}^{\infty} (n+1) \cdot \frac{1}{r^{n+2}} \cdot \sum_{m=0}^n (g_n^m \times \dots) \quad (2)$$

$$\dots \times \cos m\varphi + h_n^m \cdot \sin m\varphi) \cdot P_n^m(\cos \theta);$$

$$B_\varphi = \frac{\mu_0}{4\pi} \cdot \sum_{n=1}^{\infty} \frac{1}{r^{n+2}} \cdot \sum_{m=0}^n (g_n^m \cdot \sin m\varphi - \dots)$$

$$\dots - h_n^m \cdot \cos m\varphi) \cdot \frac{P_n^m(\cos \theta)}{\sin \theta};$$

$$B_\theta = \frac{\mu_0}{4\pi} \cdot \sum_{n=1}^{\infty} \frac{1}{r^{n+2}} \cdot \sum_{m=0}^n (g_n^m \cdot \cos m\varphi + \dots)$$

$$\dots + h_n^m \cdot \sin m\varphi) \cdot \frac{1}{\sin \theta} \cdot [(n-m+1) \times \dots$$

$$\dots \times \bar{P}_{n+1}^m(\cos \theta) - (n+1) \cdot \cos \theta \cdot P_n^m(\cos \theta)]$$

Let us first consider the case when for all N units of the microsatellite at the preliminary testing stage of magnetic cleanliness, three quantities g_{n1}^0 , g_{n1}^1 , h_{n1}^1 of the dipole component, five quantities g_{n2}^0 , g_{n2}^1 , g_{n2}^2 , h_{n2}^1 , h_{n2}^2 of the quadrupole component and seven quantities g_{n3}^0 , g_{n3}^1 , g_{n3}^2 , g_{n3}^3 , h_{n3}^1 , h_{n3}^2 , h_{n3}^3 of the

octupole component of spherical harmonics determined. Let us set the spherical coordinates r_n , φ_n and θ_n the location of all N units of the microsatellite in the spherical coordinate system associated with the magnetic center of the microsatellite.

Then the components B_{kr} , $B_{k\varphi}$, $B_{k\theta}$ of the magnetic field generated by all N units of the microsatellite at the point with coordinates r_k , φ_k and θ_k in the spherical coordinate system associated with the geometric center of the microsatellite calculated taking into account the expression for Legendre polynomials up to the third term of series based on (2) [25].

Here the coordinates r_{kn} and two angles φ_{kn} and θ_{kn} of points of calculation of the magnetic field generated by n microsatellite units in the spherical coordinate system associated with the geometric center of that N microsatellite units.

Transferred coordinates r_k , φ_k and θ_k of calculated point of components B_{kr} , $B_{k\varphi}$, $B_{k\theta}$ of the magnetic field in the spherical coordinate system associated with the geometric center of the microsatellite from the spherical coordinate system to the orthogonal system (6):

$$B_{kr} = \frac{\mu_0}{4\pi} \sum_{n=1}^N \left(\begin{aligned} &g_{n1}^0 \frac{2}{r_{kn}^3} \cos \theta_{kn} + \left[g_{n1}^1 \cos \varphi_{kn} + h_{n1}^1 \sin \varphi_{kn} \right] \frac{2}{r_{kn}^3} \sin \theta_{kn} + g_{n2}^0 \frac{3/2}{r_{kn}^4} (3 \cos^2 \theta_{kn} - 1) + \dots \\ &\dots + \left[g_{n2}^1 \cos \varphi_{kn} + h_{n2}^1 \sin \varphi_{kn} \right] \frac{9}{r_{kn}^4} \cos \theta_{kn} \sin \theta_{kn} + \left[g_{n2}^2 \cos(2\varphi_{kn}) + h_{n2}^2 \sin(2\varphi_{kn}) \right] \frac{3}{r_{kn}^4} \dots \\ &\dots * \frac{9}{r_{kn}^4} \sin^2 \theta_{kn} + g_{n3}^0 \frac{2}{r_{kn}^5} (5 \cos^3 \theta_{kn} - 3 \cos \theta_{kn}) + \left[g_{n3}^1 \cos \varphi_{kn} + h_{n3}^1 \sin \varphi_{kn} \right] \frac{6}{r_{kn}^5} \dots \\ &\dots * \frac{2}{r_{kn}^5} \sin \theta_{kn} (15 \cos^2 \theta_{kn} - 3) + \left[g_{n3}^2 \cos(2\varphi_{kn}) + h_{n3}^2 \sin(2\varphi_{kn}) \right] \frac{60}{r_{kn}^5} \cos \theta_{kn} \sin^2 \theta_{kn} + \dots \\ &\dots + \left[g_{n3}^3 \cos(3\varphi_{kn}) + h_{n3}^3 \sin(3\varphi_{kn}) \right] \frac{60}{r_{kn}^5} \sin^3 \theta_{kn} \end{aligned} \right); \quad (3)$$

$$B_{k\varphi} = \frac{\mu_0}{4\pi} \sum_{n=1}^N \left(\begin{aligned} &\left[g_{n1}^1 \sin \varphi_{kn} - h_{n1}^1 \cos \varphi_{kn} \right] \frac{1}{r_{kn}^3} \sin \theta_{kn} + \left[g_{n2}^1 \sin \varphi_{kn} - h_{n2}^1 \cos \varphi_{kn} \right] \frac{3}{r_{kn}^4} \cos \theta_{kn} + \dots \\ &\dots + \left[g_{n2}^2 \sin(2\varphi_{kn}) - h_{n2}^2 \cos(2\varphi_{kn}) \right] \frac{6}{r_{kn}^4} \sin \theta_{kn} + \left[g_{n3}^1 \sin \varphi_{kn} - h_{n3}^1 \cos \varphi_{kn} \right] \frac{1/2}{r_{kn}^5} * \dots \\ &\dots * (15 \cos^2 \theta_{kn} - 3) + \left[g_{n3}^2 \sin(2\varphi_{kn}) - h_{n3}^2 \cos(2\varphi_{kn}) \right] \frac{30}{r_{kn}^5} \cos \theta_{kn} \sin \theta_{kn} + \dots \\ &+ \left[g_{n3}^3 \sin(3\varphi_{kn}) - h_{n3}^3 \cos(3\varphi_{kn}) \right] \frac{45}{r_{kn}^5} \sin^2 \theta_{kn} \end{aligned} \right); \quad (4)$$

$$B_{k\theta} = \frac{\mu_0}{4\pi} \sum_{n=1}^N \left(\begin{aligned} &g_{n1}^0 \frac{1}{r_{kn}^3} \sin \theta_{kn} + \left[-g_{n1}^1 \cos \varphi_{kn} - h_{n1}^1 \sin \varphi_{kn} \right] \frac{1}{r_{kn}^3} \cos \theta_{kn} + \dots \\ &\dots + g_{n2}^0 \frac{3}{r_{kn}^4} \cos \theta_{kn} \sin \theta_{kn} + \left[-g_{n2}^1 \cos \varphi_{kn} - h_{n2}^1 \sin \varphi_{kn} \right] \frac{3}{r_{kn}^4} \cos(2\theta_{kn}) + \dots \\ &\dots + \left[-g_{n2}^2 \cos(2\varphi_{kn}) + h_{n2}^2 \sin(2\varphi_{kn}) \right] \frac{-6}{r_{kn}^4} \cos \theta_{kn} \sin \theta_{kn} + \dots \\ &\dots + g_{n3}^0 \frac{1/2}{r_{kn}^5} (15 \cos^2 \theta_{kn} - 3) \sin \theta_{kn} + \dots \\ &\dots + \left\{ \frac{g_{n3}^1 \cos \varphi_{kn}}{h_{n3}^1 \sin \varphi_{kn}} \right\} \frac{3/2}{r_{kn}^5} (11 \sin^2 \theta_{kn} - 4 \cos^2 \theta_{kn}) \cos \theta_{kn} + \dots \\ &\dots + \left\{ \frac{g_{n3}^2 \cos(2\varphi_{kn})}{h_{n3}^2 \sin(2\varphi_{kn})} \right\} \frac{15}{r_{kn}^5} (\sin^2 \theta_{kn} - 2 \cos^2 \theta_{kn}) \sin \theta_{kn} + \dots \\ &\dots + \left\{ \frac{g_{n3}^3 \cos(3\varphi_{kn})}{h_{n3}^3 \sin(3\varphi_{kn})} \right\} \frac{-45}{r_{kn}^5} \cos \theta_{kn} \sin^2 \theta_{kn} \end{aligned} \right); \quad (5)$$

$$z_k = r_k \cos(\theta_k), \quad x_k = r_k \cos(\varphi_k) \sin(\theta_k), \quad y_k = r_k \sin(\theta_k) \sin(\varphi_k) \quad (6)$$

Transferred coordinates r_n and two angles φ_n and θ_n location of all N units of the microsatellite from the

spherical coordinate system in the orthogonal system for the orthogonal

$$\begin{aligned} z_n &= r_n \cos(\theta_n), & x_n &= r_n \cos(\varphi_n) \sin(\theta_n), \\ y_n &= r_n \sin(\theta_n) \sin(\varphi_n). \end{aligned} \quad (7)$$

Then the coordinates r_{kn} , φ_{kn} and θ_{kn} of calculated point of components B_{kr} , $B_{k\varphi}$, $B_{k\theta}$ of the magnetic field in spherical coordinate system associated with the geometric center n unit of the microsatellite calculate

$$\begin{aligned} r_{kn} &= \sqrt{((x_k - x_n)^2 + (y_k - y_n)^2 + (z_k - z_n)^2)}; \\ \cos(\theta_{kn}) &= (z_k - z_n)/r_{kn}; \\ \text{tg}(\varphi_{kn}) &= (y_k - y_n)/(x_k - x_n). \end{aligned} \quad (8)$$

Microsatellite magnetic characteristics uncertain.

The microsatellite has completed units in its composition, which must meet the magnetic cleanliness requirements. The solar cell is potentially one of the main sources of the microsatellite magnetic field currents. To reduce the magnetic field of solar batteries, the so-called «backwiring» technique of mounting their circuits with current is used, in which the return wire from each module of the battery elements is returned under the same module along its axis line, which allows you to effectively reduce the magnetic field of the solar battery in all modes of its work [1].

The characteristics of the magnetic field of the microsatellite units do not remain constant and change depending on the microsatellite operation mode and operating time. In particular, the initial magnetic moment of the 8S3P MPS battery «SICH-2-1» spacecraft with a change in the charge current from minus 8 A to the discharge current 8 A almost linearly changed from $-0.17 \text{ A}\cdot\text{m}^2$ to $0.17 \text{ A}\cdot\text{m}^2$. Besides, antennas and components use latch springs, control valves and other moving parts magnetic characteristics of which change under different operating modes of the microsatellite.

All units with a magnetic drive (motors, linear motion converters and all other mechanisms) require independent development in terms of ensuring their magnetic cleanliness. In conclusion, we note that all spacecraft units undergo testing regarding the characteristics of their magnetic cleanliness, which must be within certain limits [19].

Let us introduce the vector \vec{G} of uncertainties of the parameters of microsatellite units magnetic cleanliness [27 – 32]. It should be noted that the values of three quantities g_{n1}^0 , g_{n1}^1 , h_{n1}^1 of the dipole component, five quantities g_{n2}^0 , g_{n2}^1 , g_{n2}^2 , h_{n2}^1 , h_{n2}^2 of the quadrupole component and seven quantities g_{n3}^0 , g_{n3}^1 , g_{n3}^2 , g_{n3}^3 , h_{n3}^1 , h_{n3}^2 , h_{n3}^3 of the octupole component of spherical harmonics for all N units of the microsatellite determined in the course of testing the magnetic purity of all microsatellite units depend on the operating modes of the microsatellite and, therefore, are functions of the components of the vector \vec{G} of uncertainties of the parameters of the magnetic purity of the microsatellite units.

Then for a given value of the vector \vec{G} of uncertainties of the parameters of the magnetic cleanliness of microsatellite units, given coordinates r_n , φ_n and θ_n of spatial arrangement of N microsatellite units with given values of three quantities $g_{n1}^0(\vec{G})$, $g_{n1}^1(\vec{G})$, $h_{n1}^1(\vec{G})$ of the dipole component, five quantities $g_{n2}^0(\vec{G})$,

$g_{n2}^1(\vec{G})$, $g_{n2}^2(\vec{G})$, $h_{n2}^1(\vec{G})$, $h_{n2}^2(\vec{G})$ of the quadrupole component and seven quantities $g_{n3}^0(\vec{G})$, $g_{n3}^1(\vec{G})$, $g_{n3}^2(\vec{G})$, $g_{n3}^3(\vec{G})$, $h_{n3}^1(\vec{G})$, $h_{n3}^2(\vec{G})$, $h_{n3}^3(\vec{G})$ of the octupole component of spherical harmonics three components $\vec{B}_{kr}(\vec{G})$, $\vec{B}_{k\varphi}(\vec{G})$, $\vec{B}_{k\theta}(\vec{G})$ of the magnetic field generated by all N units of the microsatellite at the point with coordinates r_k , φ_k and θ_k calculated based on (3) – (5). Since the results of measuring the magnetic field depend on the operating modes of the spacecraft, the components of the measurement vector $\vec{B}_{kr}(\vec{G})$, $\vec{B}_{k\varphi}(\vec{G})$, $\vec{B}_{k\theta}(\vec{G})$ also are functions of the vector \vec{G} .

Statement of the prediction problem. For design of the spatial spherical harmonics magnetic field model the methods for experimental determination of the coefficients of spatial harmonics based on the signatures of the magnetic characteristics of the tested objects during their movement or rotation relative to the measuring windings have been developed in the works [17 – 25]. With the help of such measuring windings, it is also possible to selectively measure spatial harmonics of various orders. However, this approach involves the use of measuring windings of a rather complex spatial shape, and the dimensions of such selective windings must exceed the test object when it moves through these measuring windings.

However, at present, the most common approach to building a magnetic field model is the use of many point sensors to measure the magnetic field induction generated by the test object. This approach is most widely used in the construction of a multi dipole model of the magnetic field of the test object [3 – 14]. In the ship magnetism laboratory (France), to determine the spherical harmonics of the magnetic field, when modeling the ships magnetization, a system of 39 stationary sensors is used, relative to which the test object is moved [26].

Note that today systems with point measurement of the magnetic field induction using many sensors and precision systems for moving the object under test make it possible to realize the highest accuracy in calculating the parameters of the multipole model of the magnetic field of the object under test.

Let us now consider the inverse problem of design the spatial spherical harmonics magnetic field model (3) – (5) based on the results of measurements $\vec{B}_{kr}(\vec{G})$, $\vec{B}_{k\varphi}(\vec{G})$, $\vec{B}_{k\theta}(\vec{G})$ of the microsatellite magnetic field at the K point with coordinates r_k , φ_k and θ_k by analogy with the design of a multidipole model of the magnetic field [3 – 14].

Let us introduce the vector $\vec{Y}_M(\vec{G})$, components of which are the measured values $\vec{B}_{kr}(\vec{G})$, $\vec{B}_{k\varphi}(\vec{G})$, $\vec{B}_{k\theta}(\vec{G})$ of the magnetic field at the K measurement points with the coordinates r_k , φ_k and θ_k .

Let us introduce the vector \vec{X} of the desired parameters of the mathematical model of the spacecraft magnetic field, the components of which are the desired coordinates r_n , φ_n and θ_n of spatial arrangement of N microsatellite units as well as the desired values of three quantities $g_{n1}^0(\vec{G})$, $g_{n1}^1(\vec{G})$, $h_{n1}^1(\vec{G})$ of the dipole component, five quantities $g_{n2}^0(\vec{G})$, $g_{n2}^1(\vec{G})$, $g_{n2}^2(\vec{G})$,

$h_{n2}^1(\vec{G})$, $h_{n2}^2(\vec{G})$ of the quadrupole component and seven quantities $g_{n3}^0(\vec{G})$, $g_{n3}^1(\vec{G})$, $g_{n3}^2(\vec{G})$, $g_{n3}^3(\vec{G})$, $h_{n3}^1(\vec{G})$, $h_{n3}^2(\vec{G})$, $h_{n3}^3(\vec{G})$ of the octupole component of spherical harmonics of the magnetic field generated by n units of the microsatellite at the point with coordinates r_k , φ_k and θ_k .

Let us introduce the vector $\vec{Y}_C(\vec{X}, \vec{G})$, components of which are the calculated values $\vec{B}_{kr}(\vec{G})$, $\vec{B}_{k\varphi}(\vec{G})$, $\vec{B}_{k\theta}(\vec{G})$ of the magnetic field at the K measurement points with the coordinates r_k , φ_k and θ_k .

For vector \vec{X} of the desired parameters of the mathematical model of the spacecraft magnetic field, then, based on (3) – (8) the initial nonlinear equation $\vec{Y}_C(\vec{X}, \vec{G})$ for the spacecraft multipole magnetic dipole model calculated

$$\vec{Y}_C(\vec{X}, \vec{G}) = \vec{F}(\vec{X}, \vec{G}), \quad (9)$$

where the vector nonlinear function $\vec{F}(\vec{X}, \vec{G})$ obtained on the basis of expression (3) – (8) with respect to the vector \vec{X} of unknown variables, whose components are desired coordinates r_n , φ_n and θ_n of spatial arrangement of N microsatellite units as well as the desired values of three quantities $g_{n1}^0(\vec{G})$, $g_{n1}^1(\vec{G})$, $h_{n1}^1(\vec{G})$ of the dipole component, five quantities $g_{n2}^2(\vec{G})$, $h_{n2}^1(\vec{G})$, $h_{n2}^2(\vec{G})$ of the quadrupole component and seven quantities $g_{n3}^0(\vec{G})$, $g_{n3}^1(\vec{G})$, $g_{n3}^2(\vec{G})$, $g_{n3}^3(\vec{G})$, $h_{n3}^1(\vec{G})$, $h_{n3}^2(\vec{G})$, $h_{n3}^3(\vec{G})$ of the octupole component of spherical harmonics of the magnetic field generated by n units of the microsatellite at the point with coordinates r_k , φ_k and θ_k .

Naturally that the vector nonlinear function $\vec{F}(\vec{X}, \vec{G})$ also is a function of the vector \vec{G} of uncertainties of the parameters of microsatellite units magnetic cleanliness.

Let us introduce the $\vec{E}(\vec{X}, \vec{G})$ vector of the discrepancy between the vector $\vec{Y}_M(\vec{G})$ of the measured magnetic field and the vector $\vec{Y}_C(\vec{X}, \vec{G})$ of the predicted by model (18) magnetic field

$$\vec{E}(\vec{X}, \vec{G}) = \vec{Y}_M(\vec{G}) - \vec{Y}_C(\vec{X}, \vec{G}) = \vec{Y}_M(\vec{G}) - \vec{F}(\vec{X}, \vec{G}). \quad (10)$$

We write the objective nonlinear function as the weighted sum of squared residuals between the measured and predicted by the model (23) values of the magnetic field

$$f(\vec{X}, \vec{G}) = (\vec{E}(\vec{X}, \vec{G}))^T W \vec{E}(\vec{X}, \vec{G}), \quad (11)$$

where the weight matrix W takes into account different «weights» of magnetic field measurement errors depending on the distance to the minisatellite surface.

The nonlinear objective function (11) is obtained on the basis of expression (9) with respect to the vector \vec{X} of unknown variables, whose components are the values coordinates r_n , φ_n and θ_n of spatial arrangement of N microsatellite units as well as the desired values of three quantities $g_{n1}^0(\vec{G})$, $g_{n1}^1(\vec{G})$, $h_{n1}^1(\vec{G})$ of the dipole component, five quantities $g_{n2}^0(\vec{G})$, $g_{n2}^1(\vec{G})$, $g_{n2}^2(\vec{G})$, $h_{n2}^1(\vec{G})$, $h_{n2}^2(\vec{G})$ of the quadrupole component and seven

quantities $g_{n3}^0(\vec{G})$, $g_{n3}^1(\vec{G})$, $g_{n3}^2(\vec{G})$, $g_{n3}^3(\vec{G})$, $h_{n3}^1(\vec{G})$, $h_{n3}^2(\vec{G})$, $h_{n3}^3(\vec{G})$ of the octupole component of spherical harmonics of the magnetic field generated by n units of the microsatellite at the point with coordinates r_k , φ_k and θ_k and the vector \vec{G} of uncertainties of the parameters of the magnetic cleanliness of microsatellite units.

This approach is standard when designing robust mathematical model of the spacecraft magnetic field, when the coordinates of the spatial arrangement and the magnitudes of the magnetic moments of the dipoles are found from the conditions for minimizing the vector of the discrepancy between the vector of the measured magnetic field and the vector of the predicted by model magnetic field, but for the «worst» the vector of uncertainty parameters of the spacecraft magnetic moments are found from the conditions for maximizing the same vector of the discrepancy between the vector of the measured magnetic field and the vector of the predicted by model magnetic field.

As a rule, when optimizing the nonlinear objective function (11), it is necessary to take into account restrictions on the values of coordinates r_n , φ_n and θ_n of spatial arrangement of N microsatellite units C as well as the desired values of three quantities $g_{n1}^0(\vec{G})$, $g_{n1}^1(\vec{G})$, $h_{n1}^1(\vec{G})$ of the dipole component, five quantities $g_{n2}^0(\vec{G})$, $g_{n2}^1(\vec{G})$, $g_{n2}^2(\vec{G})$, $h_{n2}^1(\vec{G})$, $h_{n2}^2(\vec{G})$ of the quadrupole component and seven quantities $g_{n3}^0(\vec{G})$, $g_{n3}^1(\vec{G})$, $g_{n3}^2(\vec{G})$, $g_{n3}^3(\vec{G})$, $h_{n3}^1(\vec{G})$, $h_{n3}^2(\vec{G})$, $h_{n3}^3(\vec{G})$ of the octupole component of spherical harmonics of the magnetic field generated by n units of the microsatellite at the point with coordinates r_k , φ_k and θ_k . These restrictions usually written as vector inequalities [31 – 36].

$$\vec{G}(\vec{X}, \vec{G}) \leq \vec{G}_{\max}. \quad (12)$$

Statement of the control problem. Consider the statement of the problem of controlling by microsatellite magnetic cleanliness based on spherical harmonics magnetic field model (3) – (5) based on the results of measurements. To ensure microsatellite magnetic cleanliness, it is necessary to install in the microsatellite space not only compensating dipoles, but also compensating quadrupole and compensating octupole to compensate for the quadrupole and octupole components of the initial magnetic field of the microsatellite. Usually, the microsatellite magnetic cleanliness requirements are presented in the form of restrictions on the total magnetic moment of the microsatellite and the magnetic field magnitude at the onboard magnetometer installation point [2, 10]. To compensate the initial microsatellite magnetic field at the onboard magnetometer installation point we introduce C magnetic units with unknown values of three quantities g_{C1}^0 , g_{C1}^1 , h_{C1}^1 of the compensating dipole component, five quantities g_{C2}^0 , g_{C2}^1 , g_{C2}^2 , h_{C2}^1 , h_{C2}^2 of the compensating quadrupole component and seven quantities g_{C3}^0 , g_{C3}^1 , g_{C3}^2 , g_{C3}^3 , h_{C3}^1 , h_{C3}^2 , h_{C3}^3 of the compensating octupole component of spherical harmonics of the magnetic field generated by C magnetic units with located at C points P_C with unknown coordinates r_c , φ_c and θ_c at the onboard magnetometer installation point.

Let us introduce the vector \vec{X} of the desired parameters for solving the problem of compensating the microsatellite initial magnetic field, whose components are the oblique values of the unknown values of three quantities $g_{C1}^0, g_{C1}^1, h_{C1}^1$ of the compensating dipole component, five quantities $g_{C2}^0, g_{C2}^1, g_{C2}^2, h_{C2}^1$ of the compensating quadrupole component and seven quantities $g_{C3}^0, g_{C3}^1, g_{C3}^2, g_{C3}^3, h_{C3}^1, h_{C3}^2, h_{C3}^3$ of the compensating octupole component of spherical harmonics of the magnetic field generated by C magnetic units with located at C points P_C with unknown coordinates r_c, φ_c and θ_c at the onboard magnetometer installation point.

Then, for a given value of the vector \vec{X} of the desired parameters of the compensating dipoles, based on (14), the vector $\vec{B}_C(\vec{X})$ of the compensating magnetic field generated by all compensating dipoles at the installation point of the onboard magnetometer generated by all compensating dipoles can be calculated [21 – 23].

Then we calculated the vector $\vec{B}_R(\vec{X}, \vec{G})$ of resulting magnetic field generated at the installation point of the onboard magnetometer by the all microsatellite units and all compensating elements

$$\vec{B}_R(\vec{X}, \vec{G}) = \vec{B}(\vec{G}) + \vec{B}_C(\vec{X}). \quad (13)$$

Then we also calculated the vector $\vec{M}_R(\vec{X}, \vec{G})$ of resulting magnetic moment

$$\vec{M}_R(\vec{X}, \vec{G}) = \vec{M}(\vec{G}) + \vec{M}_C(\vec{X}) \quad (14)$$

of all microsatellite units and all compensating elements.

Then the problem of calculated unknown values of three quantities $g_{C1}^0, g_{C1}^1, h_{C1}^1$ of the dipole component, five quantities $g_{C2}^0, g_{C2}^1, g_{C2}^2, h_{C2}^1$ of the anti-quadrupole component and seven quantities $g_{C3}^0, g_{C3}^1, g_{C3}^2, g_{C3}^3, h_{C3}^1, h_{C3}^2, h_{C3}^3$ of the anti-octupole component of spherical harmonics of the magnetic field generated by C magnetic units with located at C points P_C with unknown coordinates at the onboard magnetometer installation point of the compensating anti-quadrupole and anti-octupole can be reduced to solving the problem of minimax optimization of resulting magnetic field (13) at the onboard magnetometer installation point and resulting magnetic moment (14) of all microsatellite units and all compensating elements.

This approach is standard when designing of robust control by microsatellite magnetic cleanliness, when the coordinates of the spatial arrangement and the magnitudes of the compensating dipole, quadrupole and octupole are found from the conditions for minimizing modulus of spacecraft resulting magnetic field (13) at the magnetometer installation point and resulting magnetic moment (14) of all microsatellite units and all compensating elements for the «worst» values of the vector of uncertainty parameters of the microsatellite magnetic characteristics.

Naturally, that in this case it is necessary to take into account the restriction on the coordinates r_c, φ_c and θ_c of the spatial arrangement and quantities on anti-dipole, anti-quadrupole and on anti-octupole components in the form of inequalities (12).

In conclusion, we note that the measurement of the components of the magnetic field of the units and the

entire microsatellite assembly is usually performed in the orthogonal coordinate system. To calculate the magnetic field components B_r, B_φ, B_θ in spherical coordinates R, φ and θ according to the measured values of the magnetic field components B_x, B_y, B_z in an orthogonal coordinate system X, Y, Z we obtain the following expression

$$\begin{aligned} B_r &= B_x \sin(\theta) \cos(\varphi) + \dots \\ &\dots + B_y \sin(\theta) \sin(\varphi) + B_z \cos(\theta); \\ B_\theta &= B_x \cos(\theta) \cos(\varphi) + \dots \\ &\dots + B_y \cos(\theta) \sin(\varphi) - B_z \sin(\theta); \\ B_\varphi &= -B_x \sin(\varphi) + B_y \cos(\varphi). \end{aligned} \quad (15)$$

To calculate the magnetic field components B_x, B_y, B_z in a orthogonal coordinate system X, Y, Z according to the values of the magnetic field components B_r, B_φ, B_θ in spherical coordinates R, φ and θ we obtain the following expression

$$\begin{aligned} B_x &= B_r \sin \theta_0 \cos \varphi_0 + B_\theta \cos \theta_0 \cos \varphi_0 - \dots \\ &\dots - B_\varphi \sin \varphi_0; \\ B_y &= B_r \sin \theta_0 \sin \varphi_0 + B_\theta \cos \theta_0 \sin \varphi_0 + \dots \\ &\dots + B_\varphi \cos \varphi_0; \\ B_z &= B_r \cos \theta_0 - B_\theta \sin \theta_0. \end{aligned} \quad (16)$$

In conclusion, we note that since the strength of the magnetic field and its induction are determined from (1) by the known formulas

$$\vec{H} = -\text{grad } \vec{U}, \quad \vec{B} = \mu_0 \cdot \vec{H}, \quad (17)$$

then the magnetic field components R, φ and θ in spherical coordinates R, φ and θ , as well as the magnetic field components B_x, B_y, B_z in a orthogonal coordinate system X, Y, Z can be calculated based on the numerical differentiation of the original expression (1) for a scalar magnetic potential.

The scalar magnetic potential in the form of expression (1) is a function $U(R, \theta, \varphi)$ of three variables – spherical coordinates R, φ and θ . Therefore, the calculation of derivatives in numerical form with respect to these variables is connected with the calculation of derivatives directly from expression (1), for example, for the magnetic field components B_r , in the form

$$\frac{\partial(U(R, \theta, \varphi))}{\partial R} = \frac{U(R + \delta R, \theta, \varphi) - U(R - \delta R, \theta, \varphi)}{2\delta R}. \quad (18)$$

To calculate the magnetic field components B_x, B_y, B_z in an orthogonal coordinate system X, Y, Z first, based on the transformation of spherical coordinates R, φ and θ into orthogonal coordinate system X, Y, Z on the basis of expression (8), we represent the expression for the scalar magnetic potential (1) as a function $U(X, Y, Z)$ of three independent variables X, Y, Z , which are the orthogonal coordinate system. Then the calculation of magnetic field components B_x, B_y, B_z in an orthogonal coordinate system X, Y, Z in numerical derivatives calculation form with respect to these variables with is connected with the calculation of derivatives directly by expression (1) by analogy (18), for example, for magnetic field components B_x , in the form

$$\frac{\partial(U(X, Y, Z))}{\partial X} = \frac{U(X + \delta X, Y, Z) - U(X - \delta X, Y, Z)}{2\delta X}. \quad (19)$$

Note that when calculating the magnetic field components using expressions (3) – (5), it is required to perform 3 calculations, and when calculating the same

magnetic field components using expressions (18), (19), it is necessary to perform a calculation at 12 points, however, this uses the same expression (1) for the scalar magnetic potential.

Algorithm for solving the minimax optimization problem. To solve the problems of robust prediction and control by microsatellite magnetic cleanliness, it is necessary to solve minimax optimization problems (11), (13) and (14) with constraints (12). Consider algorithms for solving these problems. Algorithms for solving global minimax optimization problems are not trivial [37 – 42]. It is especially difficult to solve such problems, due to the need to search for a global optimum; complex landscape of the search surface, associated, among other things, with the presence of ravines; multidimensionality, multiextremality, multicriteria of problems with restrictions; lack of analytical expressions for objective functions, and, consequently, their algorithmic representation and high computational complexity, which involves the use of cumbersome numerical methods and is often a difficult independent task; non-differentiability and non-linearity; the presence of discrete and continuous variables in the goal function.

When using deterministic local search methods, a multi-start strategy is often used, which does not guarantee that the global optimum will eventually be found. Stochastic search methods are more promising for these purposes, since they explore the entire search space much more efficiently with subsequent localization in areas of local optima of the greatest interest [43 – 46].

Metaheuristic algorithms include ant colony and bee colony optimization algorithms, bacterial algorithms, particle swarm optimizations, evolutionary computations including genetic algorithms, simulated annealing method, and many others. Swarm optimization algorithms, as a kind of stochastic search method, due to their bionic features, are well suited for solving such problems [47 – 52].

The Particle Swarm Optimization (PSO) algorithm is a bionic multiagent global optimization method that models the social behavior of interacting agents [53 – 57]. The idea of the PSO method corresponds to the simulation of the movement of living beings in a flock of birds or a school of fish. Behavioral metaheuristic optimization methods are based on the bionic idea of collective adaptation, collective intelligence, i.e. the mechanism of dissemination of information in the «flock», «swarm», «school», which is due to the superiority of group intelligence over the mental abilities of one individual. The social sharing of information provides evolutionary benefits to all members of the population, and the dominance of collective intelligence is the basis for the development of PSO algorithms.

In terms of the theory of artificial intelligence, each element of the system is called an agent. In the process of finding the optimum in such methods, not one agent is involved, but their whole system, called a population. This means that the solution to the problem is sought using a multi-agent system consisting of several intelligent agents with simple rules of interaction and autonomous behavior.

The characteristic properties of objects are: communicativeness, i.e. the ability to communicate with other agents, the ability to cooperate; adaptability, i.e. adaptability to environmental conditions and the ability to learn; decentralization, simplicity of individual behavior.

These properties of agents allow the phenomenon of self-organization to manifest itself in the system when performing the task of finding an extremum. In bionic methods of metaheuristic optimization, the goal function

is more often called the fitness function, which is its synonym, but at the same time reflects the specifics of the approach used to solve the problem. Metaheuristic behavioral algorithms use a population of agents to find solutions close to optimal, checking the suitability of the current solution using a fitness function.

Agents, as a result of competition and cooperation with each other, look for a potential solution in the search space, using the value of the fitness function to improve the solution. Such methods operate on a set of potential solutions rather than a single possible solution. Each solution is incrementally improved and evaluated, with a single potential solution affecting how other solutions are improved.

Consider the PSO algorithm. In this method a swarm of particles is a set of decision points moving in space in search of a global optimum. During their movement, the particles try to improve the solution they found earlier and exchange information with their neighbors. At the initial stage of the PSO algorithm, a random initialization of a swarm of particles is performed. When performing optimization, 10–30 particles are usually sufficient. The swarm makes it possible to find the global optimum even when the number of particles in it is less than the dimension of the search space.

In the standard PSO algorithm for optimizing a swarm of particles, the speed of a swarm j particle i changes according to linear laws, in which the motion of a swarm of particles is described by the following expressions [57, 58]

$$\begin{aligned} &v_{ij}(t+1) = c_1 r_{1j}(t) \dots \\ &\dots \times [y_{ij}(t) - x_{ij}(t)] + c_2 r_{2j}(t) \dots \\ &\dots \times [y_j^*(t) - x_{ij}(t)]; \end{aligned} \quad (20)$$

$$x_{ij}(t+1) = x_{ij}(t) + v_{ij}(t+1), \quad (21)$$

where position $x_{ij}(t)$ and speed $v_{ij}(t)$ of the swarm j particle i ; positive constants c_1 and c_2 determine the weights of the cognitive and social components of the particle's velocity; random numbers $r_{1j}(t)$ and $r_{2j}(t)$ from the range [0; 1] determine the stochastic component of the particle velocity component. Here $y_{ij}(t)$ and y_j^* are the best local-best and global-gbest positions of this particle, respectively, only one particle i and all particles i of this swarm j find.

The value of the cognitive coefficient c_1 characterizes the degree of individual behavior of the particle and its desire to return to the best solution found by it earlier, while the value of the social coefficient c_2 specifies the degree of collective behavior and the desire to move towards the best solution of its neighbors.

The inertial coefficient w_j determines the influence of the particle's previous velocity on its new value. The use of the inertia coefficient makes it possible to improve the quality of the optimization process.

If, during the optimization process, the particle goes beyond the search space specified by constraints (12), then the corresponding components of its velocity are set to zero, and the particle itself returns to the nearest boundary.

The algorithm for searching for a global solution to an optimization problem can be represented as an iterative process that generates a sequence of points in accordance with a prescribed set of rules, including the termination criterion. The search for a global solution to the optimization problem occurs by enumeration of local

solutions. In the general case, it is impossible to guarantee the exact solution of the global optimization problem for multiextremely function in a finite number of steps.

To prove that the found solution is the global optimum, it is necessary to perform a complete enumeration of all possible values of the parameter vector. In most cases, this is not possible, therefore, in global optimization, it is usually not about finding the optimal one, but about finding something close to it, i.e. suboptimal solution. The preference of stochastic methods of global optimization over deterministic ones is caused by their universality, which is explained by the estimation of the values of the goal function at random points of the admissible set, followed by analysis of the results at trial points of the search space.

To increase the speed of finding a global solution, special nonlinear algorithms for stochastic multi-agent optimization have recently become widespread [58].

The PSO method, as well as its various modifications, which have shown high efficiency in single-criteria optimization, can also be used to solve optimization problems in a multi-criteria formulation. In this case, the optimization problem is formulated and solved as a vector optimization problem. When solving a vector optimization problem (13), (14), it is necessary to take into account the priority of criteria, normalize them, choose a trade-off scheme, and determine the set of Pareto optimal solutions. To solve multicriteria optimization problems, the vector criterion scalarization method can be used by aggregating particular criteria, and an acceptable solution can be searched from the set of Pareto-optimal solutions by introducing additional information about the priority of particular criteria.

One of the simplest ways to solve an optimization problem in a multicriteria setting is the method of scalar convolution of a vector optimality criterion. This approach to solving a multicriteria optimization problem allows us to reduce it to solving a single-criteria problem by aggregating particular criteria. For these purposes, in practice, linear (additive) convolution is most often used:

$$\vec{X}^* = \operatorname{argmin}_{\vec{X}} \sum_{i=1}^J \alpha_i [f_i(\vec{x})], \quad (22)$$

where α_i are weight coefficients that characterize the importance of particular criteria f_i and determine the preference for individual criteria by the decision maker.

To solve the problem of multicriteria optimization, the simplest nonlinear trade-off scheme is also often used, in which the original multicriteria problem is reduced to a single criterion

$$\vec{X}^* = \operatorname{argmin}_{\vec{X}} \sum_{i=1}^J \alpha_i [1 - y_i(\vec{x})]^{-1}, \quad (23)$$

where y_i are normalized local criteria f_i , the value of which is in the range [0; 1]. Naturally, such a formalization of the solution of the multiobjective optimization problem by reducing it to a single-objective problem allows one to reasonably choose one single point from the area of compromises – the Pareto area. However, this «single» point can be further tested in order to further improve the trade-off scheme from the point of view of the decision maker.

An alternative approach to multiobjective optimization is to search for the Pareto set, which includes all solutions that are not dominated by other solutions. To find non-dominated solutions, it is convenient to use specially calculated ranks. However, this raises the

problem of comparing several solutions that have the same rank values. To adapt the PSO method in relation to the problem of finding Pareto-optimal solutions on the set of possible values of a vector criterion, it is most simple to use binary preference relations that determine the Pareto dominance of individual solutions.

In conclusion, we note that when designing a multipole model in the form of N dipoles, it is necessary to calculate $3N$ spherical coordinates r_k , φ_k and θ_k of the location of dipoles in microsatellite space and $3N$ values $g_{n1}^0(\vec{G})$, $g_{n1}^1(\vec{G})$, $h_{n1}^1(\vec{G})$ of the components of the magnetic moments of the N dipoles. As a result, it is necessary to calculate $6N$ unknown coordinates

When designing a multipole model in the form of N multipoles with dipole, quadrupole and octupole components, it is necessary, in addition to solving the problem of designing a multipole model, to calculate another $5N$ values $g_{n2}^0(\vec{G})$, $g_{n2}^1(\vec{G})$, $g_{n2}^2(\vec{G})$, $h_{n2}^1(\vec{G})$, $h_{n2}^2(\vec{G})$ of the components of the quadrupole components, and also calculate $7N$ values $g_{n3}^0(\vec{G})$, $g_{n3}^1(\vec{G})$, $g_{n3}^2(\vec{G})$, $g_{n3}^3(\vec{G})$, $h_{n3}^1(\vec{G})$, $h_{n3}^2(\vec{G})$, $h_{n3}^3(\vec{G})$ of the components of the orthorupole components. As a result when designing a multipole model $18N$ unknown variables need calculated compared to $6N$ unknown variables in the design of the multi-dipole model.

Simulation results. Let us consider the use of the developed method for prediction and control by spacecraft magnetic cleanliness based on spatial harmonic analysis at the point of installation of the LEMI-016 magnetometer generated by the sensor of the KPNCSP, which is part of the «Potential» scientific equipment of the «Sich-2» spacecraft family to ensure the spacecraft magnetic cleanliness.

The layout of the onboard magnetometer LEMI-016 and the sensor for the KPNCSP on the «Sich-2» spacecraft family [18] shown in Fig. 2.

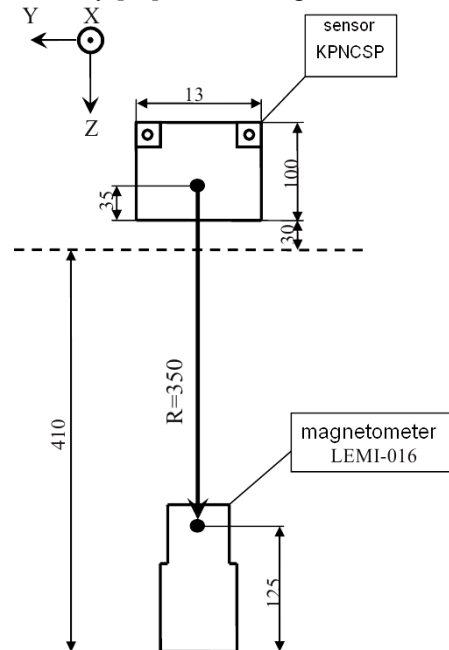


Fig. 2. The layout of the onboard magnetometer LEMI-016 and the sensor for the KPNCSP on the «Sich-2» spacecraft

To compensate the magnetic moment of the sensor, its permanent magnets are oriented antisymmetrically to

each other and a ferromagnetic screen is used. As a result, the magnetic moment of the sensor was reduced to the following values [18] of magnetic moment components in orthogonal coordinate system:

$$M_x = 0.087 \text{ A}\cdot\text{m}^2; M_y = -0.084 \text{ A}\cdot\text{m}^2; M_z = 0.042 \text{ A}\cdot\text{m}^2.$$

When using only the dipole model, the magnetic field components in a orthogonal coordinate system created by the residual magnetic moment of the sensor in the zone of the onboard magnetometer, calculated by formula (2), have the values:

$$B_x = -203 \text{ nT}; B_y = 196 \text{ nT}; B_z = 196 \text{ nT}.$$

The paper [18] presents the values of harmonics calculated on the basis of the experimentally measured signatures of the magnetic flux of the sensor at the at the magnetic measuring stand of the Anatolii Pidhornyi Institute of Mechanical Engineering Problems of the National Academy of Sciences of Ukraine [59] when it moves through the measuring circuit

$$g_1^0 = 4.1 \cdot 10^{-3}, g_1^1 = -8.4 \cdot 10^{-2}, h_1^1 = 4.2 \cdot 10^{-2}, \\ g_2^0 = 1.411 \cdot 10^{-3}, g_3^0 = 2.5 \cdot 10^{-4}.$$

In this case, the value of the magnetic field component B_z in a orthogonal coordinate system along the axis Z at the installation point of the onboard magnetometer, taking into account only the first harmonic $B_z = 237 \text{ nT}$, taking into account only the second harmonic $B_z = 352 \text{ nT}$, and taking into account only the third harmonic $B_z = 247 \text{ nT}$. The magnitude of the resulting magnetic field when three spatial harmonics are taken into account $B_z = 836 \text{ nT}$ [18]. The relative contribution of the dipole harmonic (field of the magnetic moment) to the magnetic induction created by the sensor in the area of the onboard magnetometer is only about 20 %. The contribution of quadrupole and octupole spherical harmonics to the magnetic induction of disturbance to the on-board magnetometer is about 80 % [18].

Let us consider the solution of the problem of compensation of spatial harmonics of the initial magnetic field. As a result of solving the optimization problem, the values of the harmonics of the compensating quadrupole are calculated

$$g_2^0 = 0.0249959, g_2^1 = 0.981453, g_2^2 = 0.271729, \\ h_2^1 = 0.62818, h_2^2 = 0.620474.$$

The values of the harmonics of the compensating octupole are calculated

$$g_3^0 = 0.00160516, g_3^1 = 0.0282545, g_3^2 = 0.651052, \\ g_3^3 = -0.704719, h_3^1 = 0.0031692, \\ h_3^2 = 0.175824, h_3^3 = -1.11672.$$

And also the spherical coordinates of the spatial arrangement of the compensating quadrupole and octupole are calculated

$$r_k = 0.0768617; \varphi_k = 0.163995; \theta_k = 3.90015.$$

In this case, the following values of magnetic induction were obtained in the probe of the location of the onboard magnetometer. Initial magnetic field

$$B_x = -202,86 \text{ nT}; B_y = 195,935 \text{ nT}; B_z = 243,115 \text{ nT}.$$

Compensating magnetic field

$$B_{KX} = 202.913 \text{ nT}; B_{KY} = -195.669 \text{ nT}; B_{KZ} = -243.13 \text{ nT}.$$

The resulting magnetic field

$$B_{RX} = 0.0527476 \text{ nT}; B_{RY} = 0.26579 \text{ nT}; B_{RZ} = -0.0153575 \text{ nT}.$$

Thus, due to the installation of compensating quadrupoles and octupoles, it was possible to reduce the

level of magnetic field induction at the point of installation of the «Sich-2» spacecraft family onboard magnetometer by a factor of more than two orders.

In conclusion, we note that the implementation of compensating quadrupoles and octupoles can be performed both with the help of permanent magnets and with the help of electromagnets [21, 24]. Naturally, the technical implementation of compensating elements with the help of permanent magnets is simpler, however, when implementing compensating elements with the help of electromagnets, an additional possibility appears to increase the magnetic purity of the microsatellite when it operates in various operating modes by controlling the parameters of the compensating elements in real time.

Conclusions.

1. The method for prediction and control the microsatellite magnetic cleanliness taking into account the uncertainties of the magnetic characteristics of the microsatellite, based on calculation the magnetic field spatial spherical harmonics in the area of the onboard magnetometer installation and using compensating multipole has been developed.

2. The spatial spherical harmonics of the microsatellite magnetic field is calculated based on the solution of the nonlinear minimax optimization problem. The nonlinear objective function of this nonlinear minimax optimization problem is calculated as a weighted sum of squared residuals between the measured and predicted magnetic field levels at the measurement points. The values of the spatial spherical harmonics of compensating dipole, quadrupole and octupole, as well as the coordinates of their spatial placement inside the microsatellite to compensate the dipole, quadrupole, and octupole components of the initial magnetic field of the microsatellite, are also calculated as a solution to the nonlinear minimax optimization problem. Solutions to both nonlinear minimax optimization problems are computed based on particle swarm nonlinear optimization algorithms.

3. The developed method was used to improve the magnetic cleanliness of the «Sich-2» microsatellite. Based on calculation of spatial spherical harmonics of the magnetic field generated by the kinetic parameters sensor of the neutral component of the space plasma at the installation point of the onboard magnetometer LEMI-016 of the «Sich-2» microsatellite family, the spatial harmonics of the compensating dipole, quadrupole and octupole, as well as the coordinates of the spatial location of these compensating elements in the space of a microsatellite are calculated to compensate for quadrupole and octupole harmonics of the initial magnetic field. The use of compensating quadrupole and octupole made it possible to reduce the level of magnetic field induction of the microsatellite at the point of installation of the magnetometer by more than two orders of magnitude, which will increase its controllability in orbit.

Acknowledgments. The authors express their gratitude to the researcher Anatolii Erisov of the Department of Magnetism of Technical Objects of Anatolii Pidhornyi Institute of Mechanical Engineering Problems of the National Academy of Sciences of Ukraine for the kindly provided materials on the results of experimental measured magnetic field generated by elements and «Sich-2» spacecraft family and also for numerous discussions that allowed the authors to improve the article manuscript.

Conflict of interest. The authors declare that they have no conflicts of interest.

REFERENCES

1. Rozov V.Yu., Getman A.V., Petrov S.V. Spacecraft magnetism. *Technical Electrodynamics. Thematic issue «Problems of modern electrical engineering»*, 2010, part 2, pp. 144-147. (Rus).
2. Rozov V.Yu. Methods for reducing external magnetic fields of energy-saturated objects. *Technical Electrodynamics*, 2001, no. 1, pp. 16-20.
3. Birsan M., Holtham P., Carmen. Using global optimisation techniques to solve the inverse problem for the computation of the static magnetic signature of ships. *Defense Research Establishment Atlantic*, 9 Grove St., PO Box 1012, Dartmouth, Nova Scotia, B2Y 3Z7, Canada.
4. Acuña M.H. *The design, construction and test of magnetically clean spacecraft – a practical guide*. NASA/GSFC internal report. 2004.
5. Junge A., Marliani F. Prediction of DC magnetic fields for magnetic cleanliness on spacecraft. *2011 IEEE International Symposium on Electromagnetic Compatibility*, 2011, pp. 834-839. doi: <https://doi.org/10.1109/ISEMC.2011.6038424>.
6. Lynn G.E., Hurt J.G., Harriger K.A. Magnetic control of satellite attitude. *IEEE Transactions on Communication and Electronics*, 1964, vol. 83, no. 74, pp. 570-575. doi: <https://doi.org/10.1109/TCOME.1964.6539511>.
7. Junge A., Trougnou L., Carrubba E. Measurement of Induced Equivalent Magnetic Dipole Moments for Spacecraft Units and Components. *Proceedings ESA Workshop Aerospace EMC 2009 ESA WPP-299*, 2009, vol. 4, no. 2, pp. 131-140.
8. Mehlem K., Wiegand A. Magnetostatic cleanliness of spacecraft. *2010 Asia-Pacific International Symposium on Electromagnetic Compatibility*, 2010, pp. 936-944. doi: <https://doi.org/10.1109/APEMC.2010.5475692>.
9. Messidoro P., Braghin M., Grande M. Magnetic cleanliness verification approach on tethered satellite. *16th Space Simulation Conference: Confirming Spaceworthiness into the Next Millennium*, 1991, pp. 415-434.
10. Mehlem K., Narvaez P. Magnetostatic cleanliness of the radioisotope thermoelectric generators (RTGs) of Cassini. *1999 IEEE International Symposium on Electromagnetic Compatibility*, 1999, vol. 2, pp. 899-904. doi: <https://doi.org/10.1109/ISEMC.1999.810175>.
11. Eichhorn W.L. *Magnetic dipole moment determination by near-field analysis*. Goddard Space Flight Center. Washington, D.C., National Aeronautics and Space Administration, 1972. NASA technical note, D 6685. 87 p.
12. Matsushima M., Tsunakawa H., Iijima Y., Nakazawa S., Matsuoka A., Ikegami S., Ishikawa T., Shibuya H., Shimizu H., Takahashi F. Magnetic Cleanliness Program Under Control of Electromagnetic Compatibility for the SELENE (Kaguya) Spacecraft. *Space Science Reviews*, 2010, vol. 154, no. 1-4, pp. 253-264. doi: <https://doi.org/10.1007/s11214-010-9655-x>.
13. Boghosian M., Narvaez P., Herman R. Magnetic testing, and modeling, simulation and analysis for space applications. *2013 IEEE International Symposium on Electromagnetic Compatibility*, 2013, pp. 265-270. doi: <https://doi.org/10.1109/ISEMC.2013.6670421>.
14. Mehlem K. Multiple magnetic dipole modeling and field prediction of satellites. *IEEE Transactions on Magnetics*, 1978, vol. 14, no. 5, pp. 1064-1071. doi: <https://doi.org/10.1109/TMAG.1978.1059983>.
15. Thomsen P.L., Hansen F. Danish Ørsted Mission In-Orbit Experiences and Status of The Danish Small Satellite Programme. *Annual AIAA/USU Conference on Small Satellites*, 1999, pp. SSC99-I-8.
16. Droughts S.A., Fedorov O.P. Space project Ionosat-Micro. Monograph. Kyiv, Akadempriodika Publ., 2013. 218 p. (Rus).
17. Getman A.V. *Analysis and synthesis of the magnetic field structure of technical objects on the basis of spatial harmonics*. Dissertation thesis for the degree of Doctor of Technical Sciences. Kharkiv, 2018. 43 p. (Ukr).
18. Getman A.V. Spatial harmonic analysis of the magnetic field of the sensor of the neutral plasma component. *Eastern European Journal of Advanced Technologies*, 2010, vol. 6, no. 5(48), pp. 35-38. doi: <https://doi.org/10.15587/1729-4061.2010.3326>.
19. ECSS-E-HB-20-07A. *Space engineering: Electromagnetic compatibility hand-book*. ESA-ESTEC. Requirements & Standards Division. Noordwijk, Netherlands, 2012. 228 p.
20. Rozov V.Yu. Mathematical model of electrical equipment as a source of external magnetic field. *Technical Electrodynamics*, 1995, no. 2, pp. 3-7. (Rus).
21. Rozov V.Yu., Dobrodeev P.N., Volokhov S.A. Multipole model of a technical object and its magnetic center. *Technical Electrodynamics*, 2008, no. 2, pp. 3-8. (Rus).
22. Rozov V.Yu. Selective compensation of spatial harmonics of the magnetic field of energy-saturated objects. *Technical Electrodynamics*, 2002, no. 1, pp. 8-13. (Rus).
23. Rozov V.Y., Reutskiy S.Y., Pelevin D.Y., Yakovenko V.N. The research of magnetic field of high-voltage AC transmissions lines. *Technical Electrodynamics*, 2012, no. 1, pp. 3-9. (Rus).
24. Volokhov S.A., Dobrodeev P.N., Ivleva L.F. Spatial harmonic analysis of the external magnetic field of a technical object. *Technical Electrodynamics*, 1996, no. 2, pp. 3-8. (Rus).
25. Getman A. Ensuring the Magnetic Compatibility of Electronic Components of Small Spacecraft. *2022 IEEE 3rd KhPI Week on Advanced Technology (KhPIWeek)*, 2022, no. 1-4. doi: <https://doi.org/10.1109/KhPIWeek57572.2022.9916339>.
26. Chadebec O., Rouve L.-L., Coulomb J.-L. New methods for a fast and easy computation of stray fields created by wound rods. *IEEE Transactions on Magnetics*, 2002, vol. 38, no. 2, pp. 517-520. doi: <https://doi.org/10.1109/20.996136>.
27. Rozov V.Y., Pelevin D.Y., Kundius K.D. Simulation of the magnetic field in residential buildings with built-in substations based on a two-phase multi-dipole model of a three-phase current conductor. *Electrical Engineering & Electromechanics*, 2023, no. 5, pp. 87-93. doi: <https://doi.org/10.20998/2074-272X.2023.5.13>.
28. Rozov V.Yu., Kundius K.D., Pelevin D.Ye. Active shielding of external magnetic field of built-in transformer substations. *Electrical Engineering & Electromechanics*, 2020, no. 3, pp. 24-30. doi: <https://doi.org/10.20998/2074-272x.2020.3.04>.
29. Martynenko G. Analytical Method of the Analysis of Electromagnetic Circuits of Active Magnetic Bearings for Searching Energy and Forces Taking into Account Control Law. *2020 IEEE KhPI Week on Advanced Technology (KhPIWeek)*, 2020, pp. 86-91. doi: <https://doi.org/10.1109/KhPIWeek51551.2020.9250138>.
30. Martynenko G., Martynenko V. Rotor Dynamics Modeling for Compressor and Generator of the Energy Gas Turbine Unit with Active Magnetic Bearings in Operating Modes. *2020 IEEE Problems of Automated Electrodrive. Theory and Practice (PAEP)*, 2020, pp. 1-4. doi: <https://doi.org/10.1109/PAEP49887.2020.9240781>.
31. Ostroverkhov M., Trinchuk D. Increasing the Efficiency of Electric Vehicle Drives with Supercapacitors in Power Supply. *2020 IEEE 7th International Conference on Energy Smart Systems (ESS)*, 2020, pp. 258-261. doi: <https://doi.org/10.1109/ESS50319.2020.9160291>.
32. Ostroverkhov N., Buryk N. Control System with Field Weakening of Synchronous Motor Drive. *2020 IEEE Problems of Automated Electrodrive. Theory and Practice (PAEP)*, 2020, pp. 1-5. doi: <https://doi.org/10.1109/PAEP49887.2020.9240903>.
33. Chen C.S., Reutskiy S.Y., Rozov V.Y. The method of the fundamental solutions and its modifications for electromagnetic field problems. *Computer Assisted Mechanics and Engineering Sciences*, 2009, vol. 16, no. 1, pp. 21-33.
34. Tytiuk V., Chorny O., Baranovskaya M., Serhienko S., Zachepa I., Tsvirkun L., Kuznetsov V., Tryputen N. Synthesis of a fractional-order $PI^{\lambda}D^{\mu}$ -controller for a closed system of switched reluctance motor control. *Eastern-European Journal of Enterprise Technologies*, 2019, no. 2 (98), pp. 35-42. doi: <https://doi.org/10.15587/1729-4061.2019.160946>.
35. Zagirnyak M., Serhienko S., Chorny O. Innovative technologies in laboratory workshop for students of technical specialties. *2017 IEEE First Ukraine Conference on Electrical and Computer Engineering (UKRCON)*, 2017, pp. 1216-1220. doi: <https://doi.org/10.1109/UKRCON.2017.8100446>.
36. Chorny O., Serhienko S. A virtual complex with the parametric adjustment to electromechanical system parameters. *Technical Electrodynamics*, 2019, pp. 38-41. doi: <https://doi.org/10.15407/teched2019.01.038>.
37. Shchur I., Kasha L., Bukavyn M. Efficiency Evaluation of Single and Modular Cascade Machines Operation in Electric Vehicle. *2020 IEEE 15th International Conference on Advanced Trends in Radioelectronics, Telecommunications and Computer Engineering (TCSET)*, Lviv-Slavske, Ukraine, 2020, pp. 156-161. doi: <https://doi.org/10.1109/tcset49122.2020.235413>.
38. Shchur I., Turkovskiy V. Comparative Study of Brushless DC Motor Drives with Different Configurations of Modular Multilevel Cascaded Converters. *2020 IEEE 15th International Conference on Advanced Trends in Radioelectronics, Telecommunications and Computer Engineering (TCSET)*, Lviv-Slavske, Ukraine, 2020, pp. 447-451. doi: <https://doi.org/10.1109/tcset49122.2020.235473>.

39. Solomentsev O., Zaliskyi M., Averyanova Y., Ostroumov I., Kuzmenko N., Sushchenko O., Kuznetsov B., Nikitina T., Tserne E., Pavlikov V., Zhyla S., Dergachov K., Havrylenko O., Popov A., Volosyuk V., Ruzhentsev N., Shmatko O. Method of Optimal Threshold Calculation in Case of Radio Equipment Maintenance. *Data Science and Security. Lecture Notes in Networks and Systems*, 2022, vol. 462, pp. 69-79. doi: https://doi.org/10.1007/978-981-19-2211-4_6.
40. Ruzhentsev N., Zhyla S., Pavlikov V., Volosyuk V., Tserne E., Popov A., Shmatko O., Ostroumov I., Kuzmenko N., Dergachov K., Sushchenko O., Averyanova Y., Zaliskyi M., Solomentsev O., Havrylenko O., Kuznetsov B., Nikitina T. Radio-Heat Contrasts of UAVs and Their Weather Variability at 12 GHz, 20 GHz, 34 GHz, and 94 GHz Frequencies. *ECTI Transactions on Electrical Engineering, Electronics, and Communications*, 2022, vol. 20, no. 2, pp. 163-173. doi: <https://doi.org/10.37936/ecti-ec.2022202.246878>.
41. Havrylenko O., Dergachov K., Pavlikov V., Zhyla S., Shmatko O., Ruzhentsev N., Popov A., Volosyuk V., Tserne E., Zaliskyi M., Solomentsev O., Ostroumov I., Sushchenko O., Averyanova Y., Kuzmenko N., Nikitina T., Kuznetsov B. Decision Support System Based on the ELECTRE Method. *Data Science and Security. Lecture Notes in Networks and Systems*, 2022, vol. 462, pp. 295-304. doi: https://doi.org/10.1007/978-981-19-2211-4_26.
42. Shmatko O., Volosyuk V., Zhyla S., Pavlikov V., Ruzhentsev N., Tserne E., Popov A., Ostroumov I., Kuzmenko N., Dergachov K., Sushchenko O., Averyanova Y., Zaliskyi M., Solomentsev O., Havrylenko O., Kuznetsov B., Nikitina T. Synthesis of the optimal algorithm and structure of contactless optical device for estimating the parameters of statistically uneven surfaces. *Radioelectronic and Computer Systems*, 2021, no. 4, pp. 199-213. doi: <https://doi.org/10.32620/reks.2021.4.16>.
43. Volosyuk V., Zhyla S., Pavlikov V., Ruzhentsev N., Tserne E., Popov A., Shmatko O., Dergachov K., Havrylenko O., Ostroumov I., Kuzmenko N., Sushchenko O., Averyanova Yu., Zaliskyi M., Solomentsev O., Kuznetsov B., Nikitina T. Optimal Method for Polarization Selection of Stationary Objects Against the Background of the Earth's Surface. *International Journal of Electronics and Telecommunications*, 2022, vol. 68, no. 1, pp. 83-89. doi: <https://doi.org/10.24425/ijet.2022.139852>.
44. Halchenko V., Trembovetska R., Tychkov V., Storchak A. Nonlinear surrogate synthesis of the surface circular eddy current probes. *Przegląd Elektrotechniczny*, 2019, vol. 95, no. 9, pp. 76-82. doi: <https://doi.org/10.15199/48.2019.09.15>.
45. Halchenko V.Ya., Storchak A.V., Trembovetska R.V., Tychkov V.V. The creation of a surrogate model for restoring surface profiles of the electrophysical characteristics of cylindrical objects. *Ukrainian Metrological Journal*, 2020, no. 3, pp. 27-35. doi: <https://doi.org/10.24027/2306-7039.3.2020.216824>.
46. Zhyla S., Volosyuk V., Pavlikov V., Ruzhentsev N., Tserne E., Popov A., Shmatko O., Havrylenko O., Kuzmenko N., Dergachov K., Averyanova Y., Sushchenko O., Zaliskyi M., Solomentsev O., Ostroumov I., Kuznetsov B., Nikitina T. Practical imaging algorithms in ultra-wideband radar systems using active aperture synthesis and stochastic probing signals. *Radioelectronic and Computer Systems*, 2023, no. 1, pp. 55-76. doi: <https://doi.org/10.32620/reks.2023.1.05>.
47. Chyistiakov P., Chorni O., Zhaatikov B., Sivyakova G. Remote control of electromechanical systems based on computer simulators. *2017 International Conference on Modern Electrical and Energy Systems (MEES)*, Kremenchuk, Ukraine, 2017, pp. 364-367. doi: <https://doi.org/10.1109/mees.2017.8248934>.
48. Zagimyak M., Bisikalo O., Chorna O., Chorni O. A Model of the Assessment of an Induction Motor Condition and Operation Life, Based on the Measurement of the External Magnetic Field. *2018 IEEE 3rd International Conference on Intelligent Energy and Power Systems (IEPS)*, Kharkiv, 2018, pp. 316-321. doi: <https://doi.org/10.1109/ieps.2018.8559564>.
49. Maksymenko-Sheiko K.V., Sheiko T.I., Lisin D.O., Petrenko N.D. Mathematical and Computer Modeling of the Forms of Multi-Zone Fuel Elements with Plates. *Journal of Mechanical Engineering*, 2022, vol. 25, no. 4, pp. 32-38. doi: <https://doi.org/10.15407/pmach2022.04.032>.
50. Hontarovskiy P.P., Smetankina N.V., Ugrimov S.V., Garmash N.H., Melezhyk I.I. Computational Studies of the Thermal Stress State of Multilayer Glazing with Electric Heating. *Journal of Mechanical Engineering*, 2022, vol. 25, no. 1, pp. 14-21. doi: <https://doi.org/10.15407/pmach2022.02.014>.
51. Kostikov A.O., Zevin L.I., Krol H.H., Vorontsova A.L. The Optimal Correcting the Power Value of a Nuclear Power Plant Power Unit Reactor in the Event of Equipment Failures. *Journal of Mechanical Engineering*, 2022, vol. 25, no. 3, pp. 40-45. doi: <https://doi.org/10.15407/pmach2022.03.040>.
52. Rusanov A.V., Subotin V.H., Khoryev O.M., Bykov Y.A., Korotaiev P.O., Ahibalov Y.S. Effect of 3D Shape of Pump-Turbine Runner Blade on Flow Characteristics in Turbine Mode. *Journal of Mechanical Engineering*, 2022, vol. 25, no. 4, pp. 6-14. doi: <https://doi.org/10.15407/pmach2022.04.006>.
53. Ummels M. *Stochastic Multiplayer Games Theory and Algorithms*. Amsterdam University Press, 2010. 174 p.
54. Shoham Y., Leyton-Brown K. *Multiagent Systems: Algorithmic, Game-Theoretic, and Logical Foundations*. Cambridge University Press, 2009. 504 p.
55. Sushchenko O., Averyanova Y., Ostroumov I., Kuzmenko N., Zaliskyi M., Solomentsev O., Kuznetsov B., Nikitina T., Havrylenko O., Popov A., Volosyuk V., Shmatko O., Ruzhentsev N., Zhyla S., Pavlikov V., Dergachov K., Tserne E. Algorithms for Design of Robust Stabilization Systems. *Computational Science and Its Applications – ICCSA 2022. ICCSA 2022. Lecture Notes in Computer Science*, 2022, vol. 13375, pp. 198-213. doi: https://doi.org/10.1007/978-3-031-10522-7_15.
56. Zhyla S., Volosyuk V., Pavlikov V., Ruzhentsev N., Tserne E., Popov A., Shmatko O., Havrylenko O., Kuzmenko N., Dergachov K., Averyanova Y., Sushchenko O., Zaliskyi M., Solomentsev O., Ostroumov I., Kuznetsov B., Nikitina T. Statistical synthesis of aerospace radars structure with optimal spatio-temporal signal processing, extended observation area and high spatial resolution. *Radioelectronic and Computer Systems*, 2022, no. 1, pp. 178-194. doi: <https://doi.org/10.32620/reks.2022.1.14>.
57. Xin-She Yang, Zhihua Cui, Renbin Xiao, Amir Hossein Gandomi, Mehmet Karamanoglu. *Swarm Intelligence and Bio-Inspired Computation: Theory and Applications*, Elsevier Inc., 2013. 450 p.
58. Hashim F.A., Hussain K., Houssein E.H., Mabrouk M.S., Al-Atabany W. Archimedes optimization algorithm: a new metaheuristic algorithm for solving optimization problems. *Applied Intelligence*, 2021, vol. 51, no. 3, pp. 1531-1551. doi: <https://doi.org/10.1007/s10489-020-01893-z>.
59. Baranov M.I., Rozov V.Y., Sokol Y.I. To the 100th anniversary of the National Academy of Sciences of Ukraine – the cradle of domestic science and technology. *Electrical Engineering & Electromechanics*, 2018, no. 5, pp. 3-11. doi: <https://doi.org/10.20998/2074-272X.2018.5.01>.

Received 30.08.2023

Accepted 28.10.2023

Published 02.01.2024

B.I. Kuznetsov¹, Doctor of Technical Science, Professor,

T.B. Nikitina², Doctor of Technical Science, Professor,

I.V. Bovdii¹, PhD, Senior Research Scientist,

K.V. Chunikhin¹, PhD, Research Scientist,

V.V. Kolomiets², PhD, Assistant Professor,

B.B. Kobylianskyi², PhD, Associate Professor,

¹ Anatolii Pidhornyi Institute of Mechanical Engineering

Problems of the National Academy of Sciences of Ukraine,

2/10, Pozharskogo Str., Kharkiv, 61046, Ukraine,

e-mail: kuznetsov.boris.i@gmail.com (Corresponding Author)

² Educational scientific professional pedagogical Institute of

Ukrainian Engineering Pedagogical Academy,

9a, Nosakov Str., Bakhmut, Donetsk Region, 84511, Ukraine,

e-mail: nnpipiua@ukr.net

How to cite this article:

Kuznetsov B.I., Nikitina T.B., Bovdii I.V., Chunikhin K.V., Kolomiets V.V., Kobylianskyi B.B. Method for prediction and control by uncertain microsatellite magnetic cleanliness based on calculation and compensation magnetic field spatial harmonics. *Electrical Engineering & Electromechanics*, 2024, no. 1, pp. 23-33. doi: <https://doi.org/10.20998/2074-272X.2024.1.04>